 CMES, vol.116, no.3, pp.407-431, 2018

Spline Fictitious Boundary Element Alternating Method for Edge Crack Problems with Mixed Boundary Conditions

Z. Xu[1], M. Chen[1] and X. M. Fan[1, 2, *]

Abstract: The alternating method based on the fundamental solutions of the infinite domain containing a crack, namely Muskhelishvili's solutions, divides the complex structure with a crack into a simple model without crack which can be solved by traditional numerical methods and an infinite domain with a crack which can be solved by Muskhelishvili's solutions. However, this alternating method cannot be directly applied to the edge crack problems since partial crack surface of Muskhelishvili's solutions is located outside the computational domain. In this paper, an improved alternating method, the spline fictitious boundary element alternating method (SFBEAM), based on infinite domain with the combination of spline fictitious boundary element method (SFBEM) and Muskhelishvili's solutions is proposed to solve the edge crack problems. Since the SFBEM and Muskhelishvili's solutions are obtained in the framework of infinite domain, no special treatment is needed for solving the problem of edge cracks. Different mixed boundary conditions edge crack problems with varies of computational parameters are given to certify the high precision, efficiency and applicability of the proposed method compared with other alternating methods and extend finite element method.

Keywords: Spline fictitious boundary element alternating method, mixed boundary conditions, edge crack problem, Muskhelishvili's solutions, stress intensity factor.

1 Introduction

Cracks exist in structures because of manufacture, usage, or the defects of material. Therefore, fracture mechanics plays an important role in engineering practice, such as aeronautics, astronautics and machinery manufacturing. Stress intensity factor is the most critical problem in fracture mechanics, but only a few cases can get the closed-form solution of stress intensity factor (SIF). So, numerical methods are the most common methods for solving crack problems. The finite element method (FEM) is widely used because of its strong adaptability, but more elements are set up at the crack tips due to the severe stress gradient, reducing the accuracy and efficiency of the method greatly. In order to solve the fracture problems efficiently, an improved finite element method,

[1] School of Civil Engineering and Transportation, South China University of Technology, Guangzhou, China.

[2] State Key Laboratory of Subtropical Building Science, South China University of Technology, Guangzhou, China.

[*] Corresponding Author: X. M. Fan. E-mail: fanxm@scut.edu.cn.

extended finite element method (XFEM) [Pathak, Singh and Singh (2013)], is proposed. The extended finite element method does not need to mesh the geometric or physical interfaces inside the structure, so it can overcome the difficulties caused by the high-density mesh generation at the crack tip. However, the shape function used by XFEM makes it easy to approach the linear correlation, which greatly increases the difficulty of the algebraic equation convergence. The boundary element method (BEM) [Wünsche, García-Sánchez, Sáez et al. (2010)] is also used commonly in the analysis of fracture mechanics as only the boundary needs to be discretized. However, it needs to add more elements close to the crack tips, which make it time-consuming.

Compared with the above numerical methods which are conducted to solve one crack problem, the alternating method is proposed to solve crack problems effectively using the combination of two different simple problems. The principle of the alternating method is to decompose a finite problem with a crack into the problem without crack and the infinite problem with a crack, and after that those two different problems are solved, respectively. Without the crack tip processing, this method can greatly improve the solving efficiency. Applications of the alternating method in the fracture mechanics involves the multi-crack problem [Chen (2011); Chen and Wang (2012); Chen and Wang (2014); Chen (2014)], surface elliptical cracks in 3-D bodies [Shah and Kobayashi (1973); Thresher and Smith (1972)] and surface crack of pump shaft [Chen, Kuo and Shvarts (1993)].

The infinite problem with a crack can be solved by using boundary integral equation or the fundamental solutions with a crack (Muskhelishvili's solutions). Compared with the Muskhelishvili's solutions which are derived from the mathematical method, it is lower accurate to solve the infinite problem with a crack by the boundary integral equation which bring more numerical errors. On the other hand, the problem without the crack can be conducted by using the FEM or direct BEM. The finite element alternating method (FEAM) is widely used due to its good applicability, including prediction of fatigue crack growth life of 3D model [Wang, Haynes, Huang et al. (2015); Nikishkov, Park and Atluri (2001); Tian, Dong, Bhavanam et al. (2014); Tian, Dong, Phan et al. (2015)], surface crack analysis of cylinder [Kamaya and Nishioka (2005)], simulation of surface crack and full thickness crack propagation [Park and Nikishkov (2011)] and crack simulation and analysis of countersunk rivets [Shi and Li (2006)]. In addition, the direct BEM is applied to solve the problem without crack. The BEM is attractive since only the boundaries of the problem for this method need to be modeled and hence, modeling effort is considerably reduced. Rajiyah et al. [Rajiyah and Atluri (1988)] use the direct boundary element alternating method (BEAM) to solve the SIF and the weight function of the 2D mixed crack problem. Raju et al. [Raju and Krishnamurthy (1992)] carried out detailed calculation steps of the method and calculated the SIF of the 2D mixed crack problem. Ting et al. [Ting, Chang and Yang (1995); Ting, Chen and Yang (1999); Chen, Ting and Yang (2000)] apply this method to the analysis of the third kinds of multi crack problems and the analysis of two-dimensional plate with holes.

In the edge crack problem, since the crack face tractions in Muskhelishvili's solutions are defined on the entire embedded plane with the whole crack with two crack tips, it is necessary to define tractions over the entire plane, including the fictitious tractions on the crack face defined outside the finite domain, as shown in Fig. 1. However, the FEM and

the direct BEM, which are based on the finite domain, cannot calculate the fictitious tractions on the crack outside the finite domain, so the FEAM and the BEAM cannot be directly applied in edge crack problem. In order to overcome this difficulty, Rajiyah et al. [Rajiyah and Atluri (1988)] assumed that there is a mirror image between the outside fictitious tractions and the inside tractions, as shown in Fig. 1(a), namely mirroring method. Besides, constant tractions or linear tractions are arranged on the fictitious crack by Raju et al. [Raju and Krishnamurthy (1992)], as shown in Fig. 1(b), namely uniform stresses method. However, the selection of tractions is arbitrary, which will affect the convergence of the equations related to the accuracy of the results.

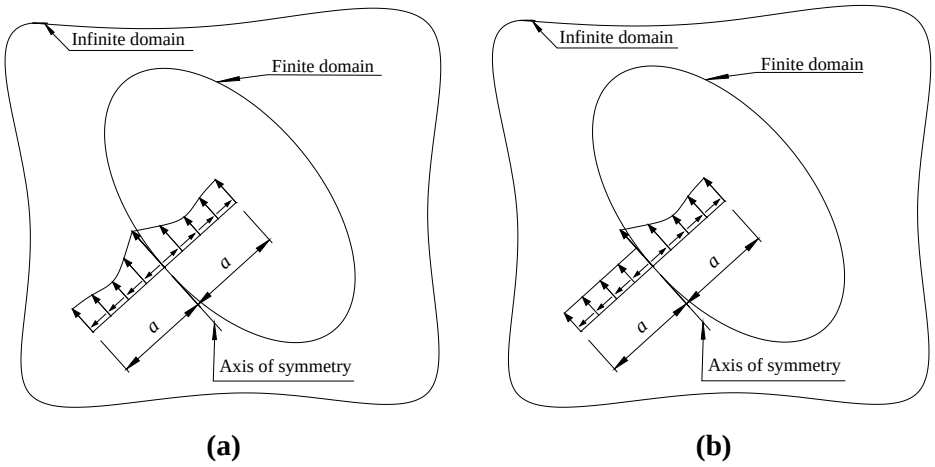

Figure 1: Treatment of edge crack

For solving the edge crack problems efficiently by the alternating method, an improved alternating method, the spline fictitious boundary element alternating method (SFBEAM) [Chen, Xu and Fan (2018)], based on an indirect BEM, spline fictitious boundary element method (SFBEM) [Su, Qin and Fan (2016); Xu, Su and Guan (2018)], and Muskhelishvili's solutions is applied in this research. Firstly, a computational model for an edge crack problem based on an infinite domain is given and then divided into two infinite domain problems by alternating method including one without a crack and another with a crack. Then, the SFBEM is used to solve the first problem and Muskhelishvili's solutions are introduced to conduct the other problem. Because the SFBEM and Muskhelishvili's solutions are formulated in the infinite domain, no special treatments are needed for solving the problem of edge crack. In the process of numerical solution, considering the distribution characteristic of the load on the crack surface, the locally thickened technique is adopted to speed up the efficiency. Finally, the SFBEAM is applied to the edge crack problem with mixed boundary conditions. Compared with other alternating methods, SFBEAM shows the high precision. Compared with the XFEM, small computational amount is needed in SFBEAM. In addition, the application of mixed boundary conditions examples show the applicability of SFBEAM.

2 SFBEAM for solving edge crack problems

2.1 Computational model of the edge crack problem based on infinite domain

A finite edge crack domain Ω is shown in Fig. 2(a). The elastic modulus, Poisson's ratio and thickness for Ω are E, υ and h, respectively. Assume the boundary of the finite domain (not including the crack surface) to be L_0. The crack surface is denoted as L_{c0}, which has a known stress boundary conditions T_0. The body forces are taken as F^l (l=1, 2).

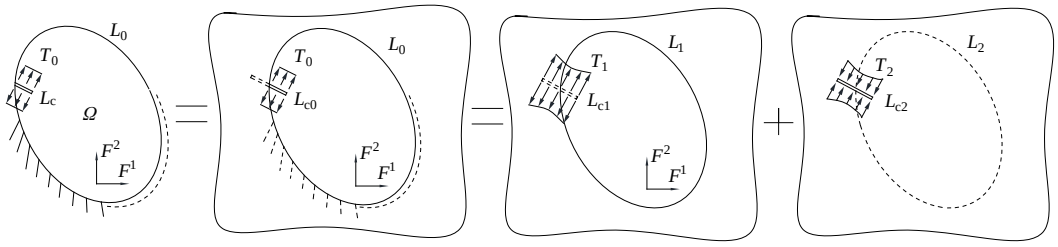

Figure 2: Superposition principle of alternating method

The governing differential equations of the plane problem represented using the displacement functions is as follows

$$\left.\begin{aligned}\frac{E}{1-\upsilon^2}\left[\frac{\partial^2 u(x,y)}{\partial x^2}+\frac{1-\upsilon}{2}\frac{\partial^2 u(x,y)}{\partial y^2}+\frac{1+\upsilon}{2}\frac{\partial^2 v(x,y)}{\partial x\partial y}\right]+F^1(x,y)=0\\ \frac{E}{1-\upsilon^2}\left[\frac{\partial^2 v(x,y)}{\partial y^2}+\frac{1-\upsilon}{2}\frac{\partial^2 v(x,y)}{\partial x^2}+\frac{1+\upsilon}{2}\frac{\partial^2 u(x,y)}{\partial x\partial y}\right]+F^2(x,y)=0\end{aligned}\right\} \tag{1}$$

where $F^1(x, y)$ and $F^2(x, y)$ are body force functions, $u(x, y)$ and $v(x, y)$ are displacements. The boundary conditions of this model including the stress boundary conditions on crack surface, the displacement boundary conditions and the stress boundary conditions in Ω are shown as below

$$\left.\begin{aligned}&\left.\begin{aligned}\sigma_\theta^{+}&=f_y^{+}\\ \tau_\theta^{+}&=f_{xy}^{+}\end{aligned}\right\}\text{the upper surface}\\ &\left.\begin{aligned}\sigma_\theta^{-}&=f_y^{-}\\ \tau_\theta^{-}&=f_{xy}^{-}\end{aligned}\right\}\text{the lower surface}\end{aligned}\right\}\ \text{Stress boundary conditions on crack surface} \tag{2}$$

$$\left.\begin{aligned}u&=\overline{u}\\ v&=\overline{v}\end{aligned}\right\}\ \text{Displacement boundary conditions} \tag{3}$$

$$\left.\begin{aligned}l\sigma_x+m\tau_{yx}&=\overline{f}_x\\ m\sigma_y+l\tau_{xy}&=\overline{f}_y\end{aligned}\right\}\ \text{Stress boundary conditions} \tag{4}$$

where σ_θ^+, τ_θ^+ and σ_θ^-, τ_θ^- are stress on the upper and lower crack surfaces, respectively, f_y^+, f_{xy}^+ and f_y^-, f_{xy}^- are the known stress distribution functions on the upper and lower crack surfaces. θ represents that the stress is the value in the local coordinates of the crack surface. u and v are displacement value on L_0, $\overline{u}$ and $\overline{v}$ are the known displacement functions on L_0. $\overline{f}_x$ and $\overline{f}_y$ are the known stress distribution function on L_0. l, m are the cosine for outer normal direction of the boundary L_0, respectively. For the mixed boundary conditions, the displacement boundary conditions and stress boundary conditions exist simultaneously.

Embedding the original problem into an infinite domain in which material properties and thickness are the same, as shown in Fig. 2(b), denoting as P_0, in which the fictitious crack surface lies outside the domain Ω. The boundary conditions and constitutive relations of Ω are the same as the original problem. According to the uniqueness theorem of the solution, the two problems in Fig. 2(a) and Fig. 2(b) have the same answer. P_0 can be decomposed into two problems including a problem embedded in an infinite non-cracked domain and an infinite cracked domain, as shown in Fig. 2(c) and Fig. 2(d), denoting as P_1 and P_2, respectively [Wang, Haynes, Huang et al. (2015)]. It is noted that these three problems are all in the infinite domain, therefore the principle of superposition can be strictly satisfied.

The boundary conditions in Ω of P_1 is L_1, The stress response at the crack location L_{c1} is T_1. In the infinite domain of P_2, the stress boundary condition at crack surface L_{c2} is T_2, and the response at the boundary location is L_2. Their governing differential equations are as follows

$$\left.\begin{aligned}
&\frac{E}{1-\upsilon^2}\left[\frac{\partial^2 u^1(x,y)}{\partial x^2}+\frac{1-\upsilon}{2}\frac{\partial^2 u^1(x,y)}{\partial y^2}+\frac{1+\upsilon}{2}\frac{\partial^2 v^1(x,y)}{\partial x\partial y}\right]+F^1(x,y)=0\\
&\frac{E}{1-\upsilon^2}\left[\frac{\partial^2 v^1(x,y)}{\partial y^2}+\frac{1-\upsilon}{2}\frac{\partial^2 v^1(x,y)}{\partial x^2}+\frac{1+\upsilon}{2}\frac{\partial^2 u^1(x,y)}{\partial x\partial y}\right]+F^2(x,y)=0
\end{aligned}\right\}\quad \text{For } P_1 \tag{5}$$

$$\left.\begin{aligned}
&\frac{E}{1-\upsilon^2}\left[\frac{\partial^2 u^2(x,y)}{\partial x^2}+\frac{1-\upsilon}{2}\frac{\partial^2 u^2(x,y)}{\partial y^2}+\frac{1+\upsilon}{2}\frac{\partial^2 v^2(x,y)}{\partial x\partial y}\right]=0\\
&\frac{E}{1-\upsilon^2}\left[\frac{\partial^2 v^2(x,y)}{\partial y^2}+\frac{1-\upsilon}{2}\frac{\partial^2 v^2(x,y)}{\partial x^2}+\frac{1+\upsilon}{2}\frac{\partial^2 u^2(x,y)}{\partial x\partial y}\right]=0
\end{aligned}\right\}\quad \text{For } P_2 \tag{6}$$

where $u^1(x, y)$and $v^1(x, y)$ are displacements of problem P_1, $u^2(x, y)$ and $v^2(x, y)$ are displacements of problem P_2.

The stress and displacement functions of problems P_0, P_1 and P_2 satisfy the following relationships [Chen (2011)]

$$\left.\begin{aligned}
\sigma_x(x,y) &= \sigma_x^1(x,y) + \sigma_x^2(x,y) \\
\sigma_y(x,y) &= \sigma_y^1(x,y) + \sigma_y^2(x,y) \\
\tau_{xy}(x,y) &= \tau_{xy}^1(x,y) + \tau_{xy}^2(x,y) \\
u(x,y) &= u^1(x,y) + u^2(x,y) \\
v(x,y) &= v^1(x,y) + v^2(x,y)
\end{aligned}\right\} \tag{7}$$

where $\sigma_x(x,y)$, $\sigma_y(x,y)$ and $\tau_{xy}(x,y)$ are stress functions in problem P_0. The superscript 1 represents the problem P_1 and the superscript 2 represents the problem P_2. The relationship between the boundary conditions of three problems is as follows

$$\left.\begin{aligned}
L_0 &= L_1 + L_2 \\
T_0 &= T_1 + T_2
\end{aligned}\right\} \tag{8}$$

2.2 SFBEM for solving infinite problem without crack

The problem P_1 is analyzed using the SFBEM. The SFBEM is a modified method for conventional indirect BEM. In SFBEM, nonsingular integral equations are first derived based on the fictitious boundary technique. Then spline functions are adopted as the trial functions for the unknown fictitious loads, and the boundary-segment-least-square technique is employed for eliminating the boundary residues. Because of these modifications, SFBEM is of high accuracy and efficiency in general. Assume that there is a fictitious boundary S outside Ω, and unknown fictitious loads X^l (l=1, 2) is applied along S, as shown in Fig. 3. The distance between the real boundary and fictitious boundary is d. Then, under the action of the fictitious loads X^l, the components of displacement and internal force at any point P_0 in the infinite domain corresponding to Ω are as follows [Su, Qin and Fan (2016)]:

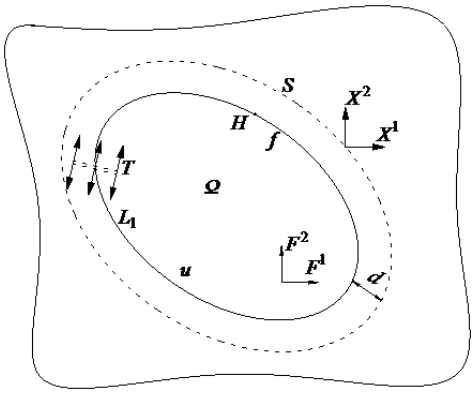

Figure 3: Finite domain and fictitious boundary

$$\left.\begin{aligned}
u^1(P_0) &= \sum_{l=1}^{2}\int_S u^l\left(H_0;Q\right)X^l\left(Q\right)\mathrm{d}s + \sum_{l=1}^{2}\iint_\Omega u^l\left(H_0;Q_0\right)F^l\left(Q_0\right)\mathrm{d}\Omega \\
v^1(P_0) &= \sum_{l=1}^{2}\int_S v^l\left(H_0;Q\right)X^l\left(Q\right)\mathrm{d}s + \sum_{l=1}^{2}\iint_\Omega v^l\left(H_0;Q_0\right)F^l\left(Q_0\right)\mathrm{d}\Omega \\
\sigma_x^1(P_0) &= \sum_{l=1}^{2}\int_S \sigma_x^l\left(H_0;Q\right)X^l\left(Q\right)\mathrm{d}s + \sum_{l=1}^{2}\iint_\Omega \sigma_x^l\left(H_0;Q_0\right)F^l\left(Q_0\right)\mathrm{d}\Omega \\
\sigma_y^1(P_0) &= \sum_{l=1}^{2}\int_S \sigma_y^l\left(H_0;Q\right)X^l\left(Q\right)\mathrm{d}s + \sum_{l=1}^{2}\iint_\Omega \sigma_y^l\left(H_0;Q_0\right)F^l\left(Q_0\right)\mathrm{d}\Omega \\
\tau_{xy}^1(P_0) &= \sum_{l=1}^{2}\int_S \tau_{xy}^l\left(H_0;Q\right)X^l\left(Q\right)\mathrm{d}s + \sum_{l=1}^{2}\iint_\Omega \tau_{xy}^l\left(H_0;Q_0\right)F^l\left(Q_0\right)\mathrm{d}\Omega
\end{aligned}\right\} \tag{9}$$

where $Q\in S$, $Q_0\in\Omega$, u^l, v^l, σ_x^l, σ_y^l and τ_{xy}^l are Kelvin's solutions (fundamental solution without crack) [Banerjee and Butterfield (1982)].

Substituting Eq. (9) into the boundary conditions along L_1, one has

$$\sum_{l=1}^{2}\int_S G_k^l(H;Q)X^l(Q)ds + \sum_{l=1}^{2}\iint_\Omega G_k^l\left(H;Q_0\right)F^l\left(Q_0\right)\mathrm{d}\Omega = L_k(H) \tag{10}$$

where $H\in L_1$; k=1, 2 represents the two boundary conditions along boundary L for plane problems; and L_k is the known boundary conditions along L_1, and G_k^l are the Kelvin's solutions. Note that the singular and hyper-singular integrals can be avoided in numerical solution because, in SFBEM, the source points and field points are not coincided. Because closed-form solutions to Eq. (10) are not available, the integral equations should be solved using a numerical basis. Divide the fictitious boundary S into M divisions as S_m (m=1, 2, ⋯, M). Then a set of B-spline functions are used to express the unknown fictitious X_m^l(s) as follow:

$$X_m^l\left(s\right) = \sum_{n=-1}^{N_m+1} x_{mn}^l\varphi_n\left(s\right) \quad \left(m=1,2,\cdots,M;l=1,2\right) \tag{11}$$

where s is the local coordinate along S_m, and N_m is the number of sub-divisions within S_m. x_{mn}^l are the unknown spline node parameters and $\varphi_n(s)$ are the third-order B-spline functions .

Substituting Eq. (11) into Eq. (10), one has the residual functions $R_k(H)$ along boundary L_1 as follows

$$R_k\left(H\right) = \sum_{l=1}^{2}\sum_{m=1}^{M}\sum_{n=-1}^{N_m+1} x_{mn}^l\int_{S_m} G_k^l\left(H;s\right)\varphi_n\left(s\right)\mathrm{d}s + \sum_{l=1}^{2}\iint_\Omega G_k^l\left(H;Q_0\right)F^l(Q_0)d\Omega - H_k\left(H\right) \quad \left(k=1,2\right) \tag{12}$$

For eliminating boundary residues $R_k(H)$, boundary L_1 is divided into N_L segments. Then let the integration of the residues along each segment equal zero, namely,

$$\int_{\Delta L_d} R_k\left(H\right)\mathrm{d}L = 0 \quad \left(k=1,2;d=1,2,\cdots,N_L\right) \tag{13}$$

where ΔL_d is the dth segment on boundary L_1.

Substitute Eq. (13) into Eq. (12), one yields

$$[A]\{X\}+\{F\}=\{L_1\} \tag{14}$$

where $\{X\}$ is the column matrix consisting of the unknown spline node parameters of the fictitious loads along S; and $[A]$ is the influence matrix of $\{X\}$ corresponding to the boundary L_1; and $\{F\}$ and $\{L_1\}$ are the known column matrices depending on the body forces within Ω and the boundary conditions along L_1, respectively.

After determining the spline node parameters $\{X\}$, the response of stress at the crack location $\{T_1\}$ can be solved as follows

$$\{T_1\}=[K]\{X\}+\{\overline{F}\} \tag{15}$$

where $[K]$ is the influence matrix of $\{X\}$ related to the crack location. $\{\overline{F}\}$ is the known body force column matrices. Since Eq. (9) is the solution to any points for the infinite domain, the response stress $\{T_1\}$ includes the stress response at the actual crack location and the stress response at the fictitious crack location.

2.3 Muskhelishvili's solutions for solving infinite cracked domain

The problem P_2 is analyzed by using Muskhelishvili's solutions. Assume an infinite cracked domain with the crack $\overline{ab}$ [Wang and Atluri (1996)] subjected to the concentrated loads f_y^+ and f_{xy}^+ at point $Q^+=d+i0^+$ at the upper crack surface and f_y^- and f_{xy}^- at point $Q^-=d+i0^-$ at the lower crack surface as shown in Fig. 4.

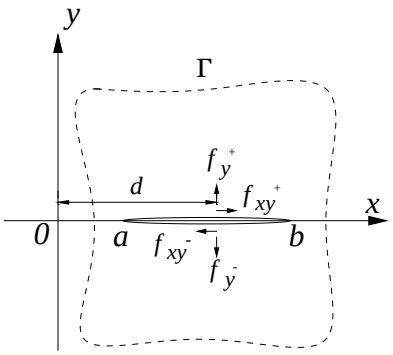

Figure 4: Crack of arbitrary length in an infinite domain

The Muskhelishvili's solutions are used to remove the crack-face cohesive stress obtained from the SFBEM solution for the alternating method. Therefore, according to Newton's third law of traction reciprocity, the concentrated load f_y and f_{xy} are the same for the upper crack surface and the lower crack surface, i.e. $f_y^+=f_y^-$, $f_{xy}^+=f_{xy}^-$. With this assumption, the stresses σ_x, σ_y and τ_{xy} and displacement u and v at any point, $z=x+iy$, can be expressed using complex functions.

$$\left.\begin{aligned}\sigma_x+\sigma_y &= 2\left[\Phi(z)+\overline{\Phi(z)}\right]\\ \sigma_y-i\tau_{xy} &= \Phi(z)+\Omega(\bar{z})+(z-\bar{z})\overline{\Phi'(z)}\end{aligned}\right\} \tag{16}$$

$$2\mu(u+iv)=\kappa w(z)-w(\bar{z})-(z-\bar{z})\overline{\Phi(z)} \tag{17}$$

$$K_I-iK_{II}=\frac{i_{ab}}{\tilde{X}(x_{ab})}\sqrt{\frac{2}{\pi(b-a)}}\boldsymbol{\Gamma}(x_{ab}) \tag{18}$$

where the stresses, displacement functions and SIF are expressed as follows

$$\left\{\begin{aligned}&\Phi(z)=\Omega(z)=\frac{\Gamma(z)}{2\pi iX(z)}\\ &\Gamma(z)=\int_L\frac{X^+(t)p(t)}{t-z}dt\\ &p(t)=f_y(t)-if_{xy}(t)\\ &\Phi'(z)=\Omega'(z)=\Omega(z)\left[\frac{1}{d-z}-\frac{(2z-a-b)}{2(z-a)(z-b)}\right]\\ &X(z)=\sqrt{z-a}\sqrt{z-b}\quad (X^+(t)\ \text{indicates the upper surface value of the funtion})\\ &w(z)=\frac{1}{\pi i}\ln\frac{\sqrt{z-d}}{\sqrt{d-a}\sqrt{z-b}-\sqrt{d-b}\sqrt{z-a}}\\ &\kappa=\begin{cases}3-4\nu & \text{plane strain}\\ \dfrac{3-\nu}{1+\nu} & \text{plane stress}\end{cases}\\ &i_{ab}=\begin{cases}i & \text{for the left crack tip } a\\ -i & \text{for the right crack tip } b\end{cases}\\ &x_{ab}=\begin{cases}a & \text{for the left crack tip } a\\ b & \text{for the right crack tip } b\end{cases}\\ &\tilde{X}(t)=\sqrt{t-a}\sqrt{t-b}\end{aligned}\right. \tag{19}$$

The response at the boundary location in problem P_2 can be determined by using Muskhelishvili's solutions as follows

$$\sum_{l=1}^{2}\int_{L_{c2}}\bar{G}_k^l(N;Q_2)T_2^l(Q_2)ds=\bar{L}_k(N) \tag{20}$$

where $Q_2\in L_{c2}$, $N\in L_2$, $\bar{L}_k$ is the stress and displacement response, and $\bar{G}_k^l$ is the Muskhelishvili's solutions.

Discretizing the integral equations Eq. (20). Non-uniform partition is used as the stress change is much more severe close to the crack tip, as shown in Fig. 5.

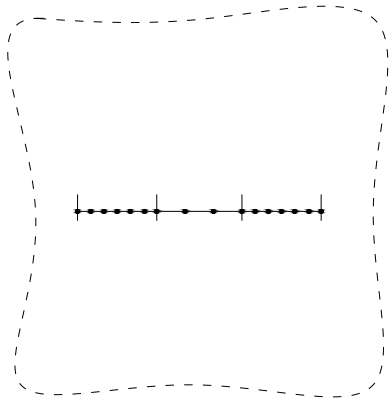

Figure 5: Non-uniform partition of crack

Let the crack L_{c2} be divided into I divisions, denoted as $L_{c2,i}$, then

$$\sum_{l=1}^{2}\sum_{i=1}^{I}\int_{L_{c2,i}} \overline{G}_{k,i}^{l}(N;Q_2)\overline{T}_{2,i}^{l}(Q_2)ds = \overline{L}_{k,i}(N) \tag{21}$$

Written in the form of matrix:

$$\{L_2\} = [\overline{K}]\{T_2\} \tag{22}$$

where $\{T_2\}$ is the column matrix containing the crack stresses. $[\overline{K}]$ is the influence matrix of $\{T_2\}$ related to the boundary location and $\{L_2\}$ is the column matrix containing the unknown stress and displacement response.

2.4 Solution of SIF by SFBEAM

An equation set consisting of Eqs. (8), (14), (15) and (22) is established. Solving this equation set, one yields

$$\{L_0\} + [\overline{K}]\{\overline{F}\} - [\overline{K}]\{T_0\} - \{F\} = ([A] - [\overline{K}][K])\{X\} \tag{23}$$

The unknown spline node parameters column matrix X can be solved from Eq. (23). Then the crack surface loading $\{T_2\}$ can be obtained. After that, the SIF can be solved directly using Muskhelishvili's solutions. Non-dimensional SIF can be solved as follow

$$F_{\mathrm{I,II}} = \frac{K_{\mathrm{I,II}}}{\sigma\sqrt{\pi a_0}} \tag{24}$$

where σ is are the uniform tensile stresses at far filed, a_0 is the crack length.

It should be noted that the crack must be at x-axis when solving the infinite problem with a crack by using Muskhelishvili's solutions. If the global coordinate is not the same as the local coordinate system, the coordinate transformations are required. In this study, the origin of the local coordinate system O', whose coordinate in the global coordinate

system is (x_0, y_0), is established at the intersection point of crack and finite domain, as shown in Fig. 6, and the included angle between the x-axis of the local coordinate system and the global coordinate system is θ (the positive rotation is counter-clockwise).

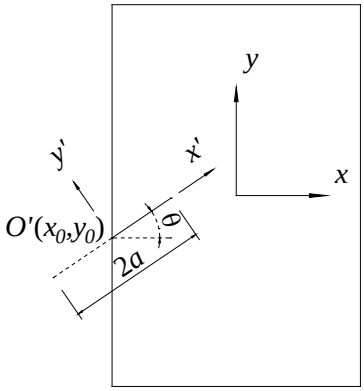

Figure 6: Transformation of overall-local coordinate

After the stress σ_x、 σ_y and τ_{xy} of the uncracked body under global coordinate system are obtained from Eq. (15), a stress transformation needs to be done to change the global stress into local stress σ'_x, σ'_y and τ'_{xy}, as shown below.

$$\begin{Bmatrix} \sigma'_x \\ \sigma'_y \\ \tau'_{xy} \end{Bmatrix} = [\lambda] \begin{Bmatrix} \sigma_x \\ \sigma_y \\ \tau_{xy} \end{Bmatrix} \tag{25}$$

where $[\lambda]$ is a transposed matrix as follow

$$[\lambda] = \begin{bmatrix} \cos^2\theta & \sin^2\theta & \sin 2\theta \\ \sin^2\theta & \cos^2\theta & -\sin 2\theta \\ -\sin\theta\cos\theta & \sin\theta\cos\theta & \cos 2\theta \end{bmatrix} \tag{26}$$

The stresses and displacements on all the boundaries of Ω are obtained from Eq. (22). Since $[\bar{K}]$ is established under the local coordinate system, so the global coordinate of L_2 must be transformed into local coordinate as follow

$$\begin{Bmatrix} x' \\ y' \end{Bmatrix} = \begin{bmatrix} \cos\theta & \sin\theta \\ -\sin\theta & \cos\theta \end{bmatrix} \begin{Bmatrix} x - x_0 \\ y - y_0 \end{Bmatrix} \tag{27}$$

where (x, y) is the global coordinate and (x', y') is the local coordinate. After Eq. (22) being solved, the stress and displacement under local coordinate system are obtained. A transformation needs to be done to change the local stress into global stress as follow

$$\begin{Bmatrix} \sigma_x \\ \sigma_y \\ \tau_{xy} \end{Bmatrix} = [\lambda]^{-1} \begin{Bmatrix} \sigma'_x \\ \sigma'_y \\ \tau'_{xy} \end{Bmatrix} \tag{28}$$

$$\begin{Bmatrix} u \\ v \end{Bmatrix} = \begin{bmatrix} \cos\theta & -\sin\theta \\ \sin\theta & \cos\theta \end{bmatrix} \begin{Bmatrix} u' \\ v' \end{Bmatrix} \tag{29}$$

3 Numerical examples

3.1 Rectangular plate with a slant single-edge crack

In practical engineering, the cracks are more likely to be appeared as mixed-mode cracks, so in this section, a rectangular plate with two opposite edges loaded, subjected to a uniformly distributed load of σ=1, as show in Fig. 7, is analyzed. The plate thickness is taken to be t=1 and Poisson's ratio of the material is assumed to be v=0.2. The modulus of elasticity is taken as E=1000 and width and height of plate are $W\times H$=10×25. There is a slant edge crack with length a above the bottom edge of plate with a height of H_1. The included angle between the crack and vertical edge of plate is β.

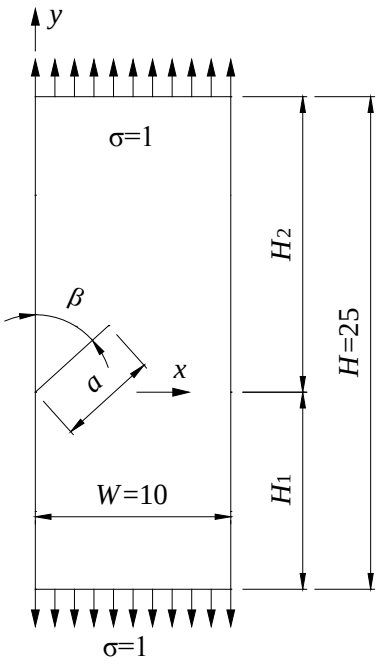

Figure 7: Rectangular plate with a slant single-edge crack

Firstly, results from the experiment [Hedan, Valle and Cottron (2010)] are used to demonstrate the accuracy of the SFBEAM. H_1 and H_2 are both taken as 12.5. β and a/W are assumed as 90° and 2.25, respectively. In the SFBEAM, 320 boundary segments, 160 fictitious boundary elements and 800 crack segments are used, as shown in Fig. 8. The non-dimensional SIF by Eq. (24) using the SFBEAM is 1.425 while the result from the

experiment in literature [Hedan, Valle and Cottron (2010)] is 1.436. The relative error compared with the experimental result is 0.77%, which indicates that the SFBEAM is of high accuracy.

Then, influence of the crack angle and crack length on SIF is investigated. Let H_1=10 and H_2=15, different lengths of crack with a/W=0.3~0.6 and different angles of crack with β=45°, β=67.5° and β=90° are considered. In order to compare the accuracy, the elements and segments of "mirroring method" and "Uniform stresses method" are the same. For the former method, the loads on the fictitious crack are symmetric with the loads on the real crack obtained by SFBEM. For the latter method, the loads on the fictitious crack are supposed to be 1. Reference solutions from Chinese Aeronautical Establishment [Chinese Aeronautical Establishment (1981)] are used. The non-dimensional SIFs calculated by Eq. (24) with a_0=a is shown in Tab. 1, Tab. 2 and Tab. 3.

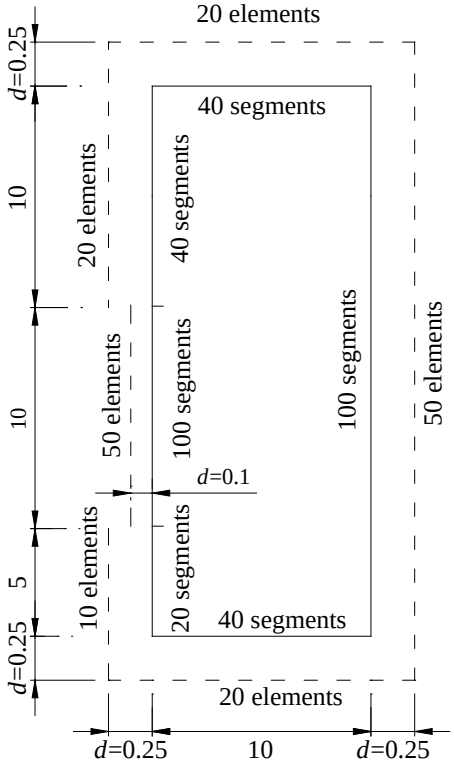

Figure 8: Layout of fictitious boundary

Table 1: Non-dimensional stress intensity factor F_I and F_{II} with different crack lengths when β=45°

Non-dimensional SIFs	*a*/*W*	Reference solutions	SFBEAM	Relative error (%)	Mirroring method	Relative error (%)	Uniform stresses method	Relative error (%)
	0.30	0.880	0.880	0.030	0.920	4.545	0.914	3.864
	0.35	0.940	0.943	0.295	0.959	2.021	0.960	2.128
	0.40	1.010	1.016	0.612	1.002	0.792	1.005	0.495
F_I	0.45	1.100	1.102	0.192	1.052	4.364	1.051	4.455
	0.50	1.190	1.203	1.065	1.107	6.975	1.095	7.983
	0.55	1.310	1.321	0.809	1.162	11.298	1.135	13.359
	0.60	1.439	1.459	1.422	1.212	15.775	1.168	18.833
	0.30	0.443	0.442	0.160	0.283	36.025	0.554	25.056
	0.35	0.473	0.469	0.848	0.301	36.364	0.573	21.142
	0.40	0.504	0.500	0.817	0.319	36.706	0.593	17.659
F_{II}	0.45	0.536	0.535	0.118	0.338	36.901	0.615	14.739
	0.50	0.571	0.576	0.888	0.358	37.303	0.637	11.559
	0.55	0.612	0.623	1.766	0.379	38.072	0.660	7.843
	0.60	0.664	0.677	1.907	0.399	39.910	0.681	2.560

Table 2: Non-dimensional stress intensity factor FI and FII with different crack lengths when β=67.5°

Non-dimensional SIFs	*a*/*W*	Reference solutions	SFBEAM	Relative error (%)	Mirroring method	Relative error (%)	Uniform stresses method	Relative error (%)
	0.30	1.440	1.411	2.008	1.340	6.944	1.260	12.500
	0.35	1.580	1.563	1.106	1.451	8.165	1.314	16.835
	0.40	1.780	1.748	1.811	1.573	11.629	1.359	23.652
F_I	0.45	2.010	1.975	1.718	1.700	15.418	1.392	30.746
	0.50	2.280	2.258	0.969	1.829	19.781	1.412	38.070
	0.55	2.620	2.613	0.270	1.946	25.725	1.418	45.878
	0.60	3.070	3.067	0.095	2.037	33.648	1.411	54.039
	0.30	0.341	0.334	2.082	0.225	34.018	0.442	29.619
	0.35	0.370	0.364	1.622	0.241	34.865	0.456	23.243
	0.40	0.403	0.400	0.821	0.257	36.228	0.470	16.625
F_{II}	0.45	0.442	0.442	0.050	0.272	38.462	0.484	9.502
	0.50	0.494	0.493	0.119	0.286	42.105	0.498	0.810
	0.55	0.565	0.556	1.604	0.297	47.434	0.510	9.735
	0.60	0.657	0.634	3.531	0.304	53.729	0.522	20.548

Table 3: Non-dimensional stress intensity factor F_I with different crack lengths when β=90°

Non-dimensional SIFs	a/W	Reference solutions	SFBEAM	Relative error (%)	Mirroring method	Relative error (%)	Uniform stresses method	Relative error (%)
	0.30	1.680	1.651	1.749	1.604	4.524	1.203	28.393
	0.35	1.880	1.852	1.496	1.786	5.000	1.234	34.362
	0.40	2.130	2.102	1.305	2.005	5.869	1.256	41.033
F_I	0.45	2.450	2.416	1.368	2.265	7.551	1.269	48.204
	0.50	2.825	2.817	0.290	2.568	9.097	1.272	54.973
	0.55	3.300	3.337	1.121	2.911	11.788	1.269	61.545
	0.60	4.030	4.031	0.016	3.272	18.809	1.264	68.635

It can be seen from above that, the calculation results are very far from the reference solutions when using the uniform stresses to simulate the fictitious crack loads. The results by using mirroring method is better than those by using uniform stresses method, but the maximum error of F_I is still up to 18.809% and the error of F_{II} is even up to 53.729%, which means that the accuracy of the mirroring method has not been reached expected. The maximum error of results calculated by SFBEAM are only 2.008%, most of which are below 1%, proving the advantages of SFBEAM. In addition, it can be found that the relative errors of the two methods increase with the increase of the crack lengths, while the results of SFBEAM agree well with the reference solutions. What is more, it is obviously that when the length of the crack increases, the value of non-dimensional SIFs F_I and F_{II} will increase, and when the crack length remains unchanged and the angle β increases, F_I will increase and F_{II} will decrease until F_{II} to be zero when β=90°.

After discussing the influence of crack angle and crack length on the SIF, the position of the crack becomes another interesting topic. Suppose the length and angle of crack are a=4, β=45° and β=67.5°, respectively. H_1 is changed from 5 to 20 with an interval of 2.5. The above three methods are also used to solve the problem. The results are shown in Tab. 4 and Tab. 5.

It can be seen from to Tab. 4 and Tab. 5 that, the values obtained by SFBEAM agree well with those of reference solutions, while the results obtained by mirroring method and uniform stresses method have large difference. When H_1<15, the values of non-dimensional SIFs F_I and F_{II} almost show no change，but when H_1>15, the values of F_I increase sharply as H_1 increases, while the values of F_{II} decrease as H_1 increases.

Table 4: Non-dimensional stress intensity factors with different crack position when β=45°

Non-dimensional SIFs	H	Reference solutions	SFBEAM	Relative error (%)	Mirroring method	Relative error (%)	Uniform stresses method	Relative error (%)[3]
	5.00	1.018	1.016	0.149	0.996	2.115	1.047	2.898
	7.50	1.018	1.016	0.149	1.001	1.623	1.044	2.603
	10.00	1.018	1.016	0.149	1.005	1.230	1.002	1.525
	12.50	1.019	1.018	0.063	0.997	2.125	1.053	3.373
F_{I}	15.00	1.037	1.036	0.122	1.004	3.207	1.092	5.277
	16.25	1.075	1.074	0.093	1.025	4.651	1.150	6.977
	17.50	1.174	1.173	0.044	1.083	7.713	1.268	8.052
	18.75	1.418	1.419	0.071	1.197	15.585	1.542	8.745
	20.00	2.106	2.118	0.564	1.333	36.708	2.153	2.226
	5.00	0.509	0.503	1.159	0.594	16.723	0.337	33.779
	7.50	0.506	0.500	1.091	0.592	17.109	0.337	33.335
	10.00	0.506	0.500	1.091	0.593	17.306	0.319	36.896
	12.50	0.505	0.500	1.036	0.590	16.778	0.338	33.100
F_{II}	15.00	0.502	0.497	0.966	0.585	16.569	0.339	32.449
	16.25	0.496	0.491	1.008	0.577	16.331	0.336	32.258
	17.50	0.483	0.478	1.024	0.564	16.783	0.325	32.705
	18.75	0.450	0.445	1.098	0.538	19.571	0.291	35.325
	20.00	0.340	0.336	1.236	0.508	49.321	0.182	46.503

Table 5: Non-dimensional stress intensity factors with different crack position when β=67.5°

Non-dimensional SIFs	H	Reference solutions	SFBEAM	Relative error (%)	Mirroring method	Relative error (%)	Uniform stresses method	Relative error (%)
	5.00	1.760	1.759	0.072	1.387	21.205	1.631	7.344
	7.50	1.755	1.749	0.337	1.373	21.762	1.652	5.864
	10.00	1.755	1.748	0.394	1.359	22.560	1.573	10.366
	12.50	1.756	1.749	0.385	1.352	22.996	1.659	5.511
F_{I}	15.00	1.762	1.756	0.323	1.353	23.198	1.694	3.842
	16.25	1.779	1.773	0.347	1.358	23.672	1.739	2.258
	17.50	1.826	1.820	0.344	1.365	25.258	1.820	0.344
	18.75	1.948	1.937	0.572	1.378	29.266	1.983	1.789
	20.00	2.258	2.257	0.027	1.382	38.785	2.263	0.239
	5.00	0.427	0.424	0.724	0.501	17.305	0.278	34.909
	7.50	0.406	0.402	1.107	0.482	18.574	0.274	32.595
	10.00	0.404	0.400	0.911	0.470	16.430	0.257	36.335
	12.50	0.404	0.399	1.159	0.470	16.430	0.270	33.115
F_{II}	15.00	0.398	0.394	1.084	0.465	16.741	0.267	32.968
	16.25	0.388	0.383	1.258	0.459	18.335	0.261	32.711
	17.50	0.360	0.355	1.299	0.444	23.446	0.241	32.994
	18.75	0.294	0.290	1.341	0.414	40.844	0.194	34.001
	20.00	0.146	0.144	1.644	0.370	152.720	0.091	37.845

3.2 Eccentric tension square plate with an edge crack

A square plate is subjected to two uniformly distributed loads of σ=1, as show in Fig. 9. The plate thickness is assumed to be t=1. Poisson's ratio of the material and the modulus of elasticity are taken as v=0.2 and E=1000, respectively. The width and height of plate are $2b \times 2H$=20×20. There is a horizontal middle edge on the plate left edge. The distributing length of uniform loads is d.

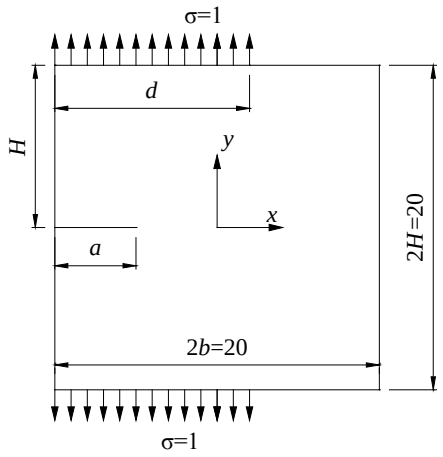

Figure 9: Eccentric tension square plate with an edge crack

The length of the uniform force distribution is considered to be $d/2b$=0.7 and $d/2b$=0.3. In each situation, different lengths of crack $a/2b$=0.1~0.8 are considered. For the purpose of investigating the efficiency of SFBEAM, the XFEM is also used, and the CPU time elapsed by the two methods is recorded respectively. Reference solutions from Chinese Aeronautical Establishment [Chinese Aeronautical Establishment (1981)] are used. Non-dimensional SIF can be solved as follow

$$F_{\mathrm{I}} = \frac{K_{\mathrm{I}}}{\sigma d\sqrt{\pi a}\ /\ 2b} \tag{30}$$

In SFBEAM, 160 boundary segments, 80 fictitious boundary elements and 800 crack segments are used, as shown in Fig. 10. In XFEM, 800×800 4-node quadrilateral elements are used. The results are shown in Tab. 6.

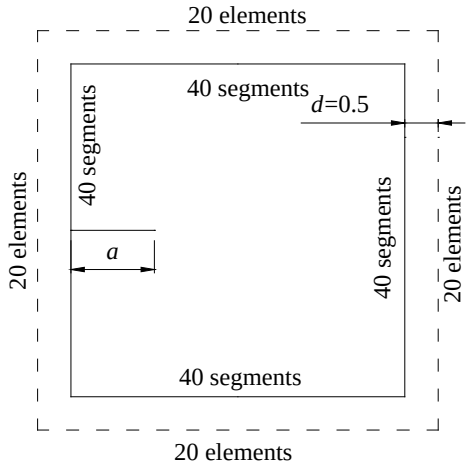

Figure 10: Layout of fictitious boundary

Table 6: Non-dimensional stress intensity factor F_I with different length of the uniform force distribution

d/2b	*a/W*	Reference solutions	SFBEAM	Relative error (%)	Computing time (s)	XFEM	Relative error (%)	Computing time (s)
0.7	0.1	1.950	1.948	0.113	10.957	1.954	0.197	43.425
	0.2	2.310	2.306	0.182	10.964	2.309	0.054	45.044
	0.3	2.820	2.816	0.146	10.966	2.817	0.124	47.295
	0.4	3.480	3.479	0.030	10.986	3.475	0.132	49.345
	0.5	4.400	4.410	0.230	11.007	4.400	0.006	52.294
	0.6	5.920	5.933	0.219	10.972	5.910	0.164	54.994
	0.7	8.880	8.914	0.380	10.961	8.863	0.196	56.314
	0.8	16.200	16.261	0.377	10.985	16.146	0.334	59.494
0.3	0.1	4.090	4.072	0.432	10.985	4.083	0.160	43.275
	0.2	4.430	4.423	0.162	10.955	4.426	0.085	44.974
	0.3	4.920	4.928	0.160	10.975	4.926	0.118	46.991
	0.4	5.520	5.571	0.919	10.955	5.572	0.947	49.571
	0.5	6.570	6.585	0.222	10.947	6.564	0.094	52.082
	0.6	8.390	8.415	0.303	10.962	8.377	0.156	54.867
	0.7	12.200	12.245	0.371	10.982	12.168	0.266	57.028
	0.8	21.800	21.896	0.441	10.950	21.734	0.303	59.782

Tab. 6 shows that the results obtained by these two methods agree well with reference solutions. The maximum error of XFEM is 0.947%, while that of SFBEAM is 0.919%. But the computing time of SFBEAM is about 11 s, while that of XFEM is more than 43 s. Besides, with the change of crack length, the computing time changes very small, shows little effect by the crack length. The XFEM has low efficiency, and the computing time increases as the crack length increases, which means the calculation time is greatly influenced by the crack length.

3.3 Square plate with an edge crack under complex boundary conditions

The accuracy of SFBEAM to solve the crack problem with mixed boundary conditions is considered in this example. A square plate with left edge fixed and right one slide-supported, subjected to a uniformly distributed load of σ=1 on top edge, as shown in Fig. 11, is analyzed. The plate thickness is taken to be t=1 and Poisson's ratio of the material is assumed to be v=0.2. The modulus of elasticity is assumed as E=1000 and the size of plate is 2W=20. There is a horizontal edge crack with length a at the middle of right edge of plate.

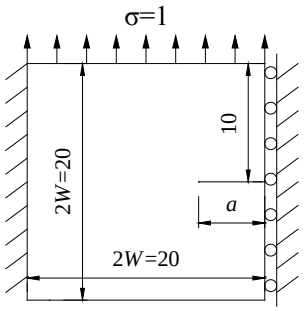

Figure 11: Square plate with an edge crack under complex boundary conditions

The length of crack is a/W=0.1~0.7. In SFBEAM, 200 boundary segments, 100 fictitious boundary elements and 1200 crack segments are used, as shown in Fig. 12. Abaqus is conducted to obtain the reference solutions of the problem, 1/4 singularity elements are used close to the crack tip and 7492 elements are taken for calculation. The results are shown in Tab. 7.

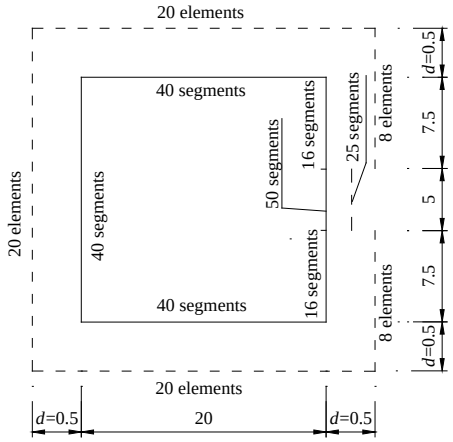

Figure 12: Layout of fictitious boundary

Table 7: Non-dimensional stress intensity factor F_I with different crack lengths

a/W	Reference solutions	SFBEAM	Relative error (%)
0.1	0.519	0.518	0.245
0.2	0.536	0.535	0.123
0.3	0.563	0.562	0.042
0.4	0.598	0.598	0.042
0.5	0.640	0.640	0.008
0.6	0.686	0.686	0.072
0.7	0.736	0.736	0.008

Tab. 7 shows that the difference of values of the SIF obtained by the two methods is very small, which proves the effectiveness of SFBEAM in solving the problems with complex

boundary condition. And high accuracy can be achieved with small degrees of freedom in SFBEAM. Therefore, the proposed method is superior to solve the crack problem than conventional FEM with lots of freedom of degrees. It can be found that, due to the constraint of the boundary displacement, the values of SIF increase slowly with the increase of the crack length.

3.4 Circular plate with a side crack subjected to uniform load

There is the horizontal edge crack loaded by constant normal σ=1 or constant shear traction τ=1 on the left of a circular plate, as shown in Fig. 13. The plate thickness is taken as t=1 and Poisson's ratio of the material is assumed to be v=0.2. The modulus of elasticity is assumed as E=1000 and the size of plate is R=10. The length of crack is a.

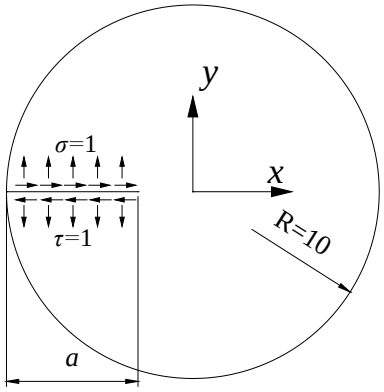

Figure 13: Circular plate with a side crack subjected to uniform load

In SFBEAM, 204 boundary segments, 102 fictitious boundary elements and 800 crack segments are used, as shown in Fig. 14. The results with different length of crack are obtained, and reference solutions from references [Chinese Aeronautical Establishment (1981)] and [Fett (2002)] are used. The results are shown in Tab. 8 and Tab. 9.

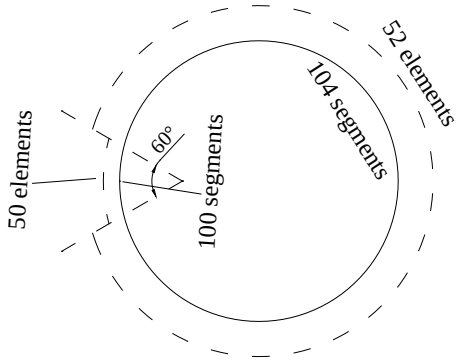

Figure 14: Layout of fictitious boundary

Table 8: Non-dimensional stress intensity factor F_I when σ=1

a/*R*	Reference solutions	SFBEAM	Relative error (%)
0.125	1.230	1.228	0.195
0.250	1.368	1.360	0.585
0.375	1.530	1.523	0.464
0.500	1.720	1.719	0.088
0.625	1.960	1.960	0.006
0.750	2.260	2.263	0.150

Table 9: Non-dimensional stress intensity factor F_{II} when τ=1

a/*R*	Reference solutions	SFBEAM	Relative error (%)
0.125	1.127	1.128	0.248
0.250	1.143	1.156	1.148
0.375	1.167	1.183	1.375
0.500	1.199	1.213	1.194
0.625	1.237	1.247	0.810
0.750	1.282	1.287	0.358

Comparing the results obtained by different methods, it is found that the maximum error of F_I is only 0.585%, and the maximum deviation of F_{II} is only 1.375%, which shows that the SFBEAM has high accuracy and is applicable to the problems with loads on the crack.

4 Conclusion

In this paper, the spline fictitious boundary element alternating method (SFBEAM) for solving the edge crack problem is presented with the combination of the SFBEM and the Muskhelishvili's solutions based on the infinite domain. Compared with other alternating methods, Because the SFBEM and Muskhelishvili's solutions are formulated in the infinite domain, no special treatments are needed for solving the problem of edge crack. Besides, with the locally thickened technique close to the crack tip meshes, the solving efficiency is improved. The SIF solutions of a rectangular plate with a slant single-edge crack and an eccentric tension square plate with an edge crack are discussed. The advantage of high precision of the SFBEAM is verified compared with other two alternative methods and the advantage of high efficiency of SFBEAM is verified compared the extended finite element method using their CPU results. In addition, the method is also applied to solve a square plate with an edge crack under mixed boundary conditions and a circular plate with a side crack subjected to uniform load on the crack surface, and the results show that the method is of high accuracy and have the strong adaptability to the mixed boundary conditions edge crack problems.

Acknowledgments: This research was supported by the National Natural Science Foundation of China (51078150), the National Natural Science Foundation of China

(11602087), the State Key Laboratory of Subtropical Building Science, South China University of Technology (2017ZB32) and National Undergraduate Innovative and Entrepreneurial Training Program (201810561180).

References

Banerjee, P. K.; Butterfield, R. (1982): Boundary element method in engineering science. *Computer Methods in Applied Mechanics and Engineering*, vol. 30, no. 1, pp. 125.

Chen, K. L.; Kuo, A. Y.; Shvarts, S. (1993): *Stress Iintensity Factor Solutions for Partial Elliptical Surface Cracks in Cylindrical Shafts*. ASTM Special Technical Publication, USA.

Chen, K. T.; Ting, K.; Yang, W. S. (2000): Stress analysis of two-dimensional perforated plates using boundary element alternating method. *Computer and Structures*, vol. 75, no. 3, pp. 515-527.

Chen, M., Xu, Z., Fan, X. M. (2018): Evaluation of the T-stress and stress intensity factor for multi-crack problem using spline fictitious boundary element alternating method. *Engineering Analysis with Boundary Elements*, vol. 94, pp. 69-78.

Chen, Y. Z. (2011): Solution of multiple crack problem in a finite plate using an alternating method based on two kinds of integral equation. *Engineering Analysis with Boundary Elements*, vol. 35, no. 10, pp. 1109-1115.

Chen, Y. Z. (2014): Evaluation of the T-stress for multiple cracks in an elastic half-plane using singular integral equation and Green's function method. *Applied Mathematics and Computation*, vol. 228, pp. 17-30.

Chen, Y. Z.; Wang, Z. X. (2012): Solution of multiple crack problem in a finite plate using coupled integral equations. *International Journal of Solids and Structures*, vol. 49, no. 1, pp. 87-94.

Chen, Y. Z.; Wang, Z. X. (2014): Evaluation of the T-stress for multiple cracks in an infinite plate using singular integral equation. *International Journal of Computational Methods*, vol. 11, no. 5.

Chinese Aeronautical Establishment (1981): *Handbook of Stress Intensity Factors*. Science Publishing Company, China. (in Chinese)

Fett, T. (2002): Stress intensity factors and T-stress for single and double-edge-cracked circular disks under mixed boundary conditions. *Engineering Fracture Mechanics*, vol. 69, pp. 69-83.

Hedan, S.; Valle, V.; Cottron, M. (2010): In plane displacement formulation for finite cracked plates under mode I using grid method and finite element analysis. *Experimental mechanics*, vol. 50, no. 2, pp. 401-412.

Kamaya, M.; Nishioka, T. (2005): Analysis of surface crack in cylinder by finite element alternating method. *Journal of Pressure Vessel Technology*, vol. 127, no. 2, pp. 165-172.

Nikishkov, G. P.; Park, J. H.; Atluri, S. N. (2001): SGBEM-FEM alternating method for analyzing 3D non-planar cracks and their growth in structural components. *Computer Modeling in Engineering and Sciences*, vol. 2, no. 3, pp. 401-422.

Park, J. H.; Nikishkov, G. P. (2011): Growth simulation for 3D surface and through-thickness cracks using SGBEM-FEM alternating method. *Journal of Mechanical Science and Technology*, vol. 25, no. 9, pp. 2335-2344.

Pathak, H.; Singh, A.; Singh, I. V. (2013): Fatigue crack growth simulations of 3-D problems using XFEM. *International Journal of Mechanical Sciences*, vol. 76, no. 11, pp. 112-131.

Rajiyah, H.; Atluri, S. N. (1989): Evaluation of *K*-factors and weight functions for 2-D mixed-mode multiple cracks by the boundary element alternating method. *Engineering Fracture Mechanics*, vol. 32, no. 6, pp. 911-922.

Raju, I. S.; Krishnamurthy, T. (1992): A boundary element alternating method for two-dimensional mixed-mode fracture problems. *Computational Mechanics*, vol. 10, no. 2, pp. 133-150.

Shah, R. C.; Kobayashi, A. S. (1973): Stress intensity factors for an elliptical crack approaching the surface of a semi-infinite solid. *International Journal of Fracture*, vol. 9, no. 2, pp. 133-146.

Shi, G.; Li, G. (2006): Modelling and analyses of cracks in fuselage lap joints with a single-countersunk rivet. *Computational Methods*, vol. 18, no. 3, pp. 1715-1725.

Su, C.; Qin, Z. S.; Fan, X. M. (2016): Stochastic spline fictitious boundary element method for modal analysis of plane elastic problems with random fields. *Engineering Analysis with Boundary Elements*, vol. 66, pp. 66-76.

Thresher, R. W.; Smith, F. W. (1972): Stress-intensity factors for a surface crack in a finite solid. *Journal of Applied Mechanics*, vol. 39, no. 1, pp. 195-200.

Tian, L. G.; Dong, L. T.; Bhavanam, S.; Phan, N.; Atluri S. N. (2014): Mixed-mode fracture & non-planar analyses of cracked I-beams, using a 3D SGBEM-FEM alternating method. *Theoretical and Applied Fracture Mechanics*, vol. 74, pp. 188-199.

Tian, L. G.; Dong, L. T.; Phan, N.; Atluri S. N. (2015): Three-dimensional SGBEM-FEM alternating method for analyzing fatigue-crack growth in and the life of attachment lugs. *Journal of Engineering Mechanics*, vol. 141, no. 4.

Ting, K.; Chang, K. K.; Yang, M. F. (1995): Analysis of Mode-III fracture problem with multiple cracks by boundary element alternating method. *International Journal of Pressure Vessels and Piping*, vol. 62, no. 3, pp. 259-267.

Ting, K.; Chen, K. T.; Yang, W. S. (1999): Boundary element alternating method applied to analyze the stress concentration problems of multiple elliptical holes in an infinite domain. *Nuclear Engineering and Design*, vol. 187, no. 3, pp. 303-313.

Wang, H. K.; Haynes, R.; Huang, H. Z.; Dong, L. T.; Atluri, S. N. (2015): The use of high-performance fatigue mechanics and the extended kalman/particle filters, foe diagnostics and prognostics of aircraft structures. *Computer Modeling in Engineering and Sciences*, vol. 105, no. 1, pp. 1-24.

Wang, L.; Atluri, S. N. (1996): Recent advances in the alternating method for elastic and inelastic fracture analyses. *Computer Methods in Applied Mechanics and Engineering*, vol. 137, pp. 1-58.

Wünsche, M.; García-Sánchez, F.; Sáez, A.; Zhang, C. (2010): A 2D time-domain collocation-Galerkin BEM for dynamic crack analysis in piezoelectric solids. *Engineering Analysis with Boundary Elements*, vol. 34, no. 4, pp. 377-387.

Xu, Z.; Su, C.; Guan, Z. W. (2018): Analysis of multi-crack problems by the spline fictitious boundary element method based on Erdogan fundamental solutions. *Acta Mechanica*, vol. 229, pp. 3257-3278.